Basrah Journal for Engineering Sciences, Vol. 21, No. 3, (2021), 10-24

Original Article

Journal homepage: www.bjes.edu.iq
ISSN (Online): 23118385, ISSN (Print): 18146120

Buckling Simulation of Simply Support FG Beam Based on Different Beam Theories

Raghad Azeez Neamah [1,*], Ameen Ahmad Nassar [2], Luay S. Alansari [3]

[1,3] *Department of Mechanical Engineering, College of Engineering, University of Kufa, Najaf, Iraq*
[2] *Department of Mechanical Engineering, College of Engineering, University of Basrah, Basrah, Iraq*
E-mail addresses: ragad.deibel@uokufa.edu.iq , ameen.nassar@uobasrah.edu.iq , luays.alansari@uokufa.edu.iq
Received: 24 July 2021; Accepted: 12 August 2021; Published: 5 October 2021

Abstract

In this paper, a new model of beam was built to study and simulate the buckling behavior of function graded beam. All equations of motion are derived using the principal of the minimum total potential energy and based on Euler-Bernoulli, first and high order shear deformation Timoshenko beam theory. The Navier solution is used for simply supported beam, and exact formulas found for buckling load. The properties of material of FG beam are assumed to change in thickness direction by using the power law formula. The dimensionless critical buckling load is calculated analytically by the FORTRAN program and numerically by ANSYS software. In the beginning, the analytical and numerical results are validated with results available in previous works and it is also has very good agreement in comparison with and some researchers. In the present study, the lower layer of the graded beam is made up of aluminum metal. As for the properties of the rest of the layers, they are calculated based on the modulus ratios studied. The effect of length to thickness ratio, modulus ratio, and power law index on the dimensionless critical buckling load of function graded beam calculating by FORTRAN and ANSYS programs are discussed. The numerical analysis of function graded beam offers accurate results and very close to the analytical solution using Timoshenko Beam theory.

Keywords: Functionally Graded Beam FGB, Buckling Analysis, Different Beam Theory, Finite Element Method.

http://dx.doi.org/10.33971/bjes.21.3.2

1. Introduction

Functionally graded beam (FGB) is a group of mixtures, in which the properties of material such as modulus of elasticity, density, poisons ratio, etc… varies in different direction, thickness, longitudinal, and in both directions respectively. Usually, FGB, consist of ceramic and metal. The ceramic can resist high thermal loading and the metal has excellent structural strength. These types of materials have been used in many fields, such as such as aerospace, mechanical, and medical sectors, to reduce the concentration and residual of stress, and to improve connection strength. In the literature, various numerical and analytical methods are proposed to analyze the buckling behavior of FG beams.

In 2007, Shariat and Eslami [1] presented buckling analysis of rectangular thick FG plates under (uniaxial, biaxial compression, and biaxial compression and tension) mechanical and thermal loads. In 2009, Metin [2] studied the buckling of nano-beam by using anon local beam theory. In 2012, Farhatnia et al. [3] employed FOSDT and GDQM for the analysis of buckling for FG thick beams. In 2013, Li et al. [4] obtainable an analytical process with various boundary conditions to find buckling loads of FG Euler and Timoshenko beams. Kien et al. [5] used the analytical solution for buckling behavior of axially loaded FGM beams. Lei et al. [6] presented the analysis of buckling for FG carbon nanotube (FG-CNTRC) plates under different in-plane mechanical loads by the method of element-free kp-Ritz. The critical buckling load of axial function graded beam by Jowita [7] in 2014 are studied. Saljooghi et al. [8] analyzed buckling load for function graded beam by using the Reproducing Kernal practical method (RKPM). In 2015 Trung-Kien et al. [9] presented a new shear deformation with higher degree for buckling analysis for isotropic and functionally graded sandwich beams.

Uysal and Kremzer [10] studied the behavior buckling of short cylindrical function graded polymetric material (FGPM s). Vo et al. [11] developed a three-dimension theory to analysis the buckling of functionally graded sandwich beams. In 2016, the behaviour of buckling of post-buckling of multilayer function graded nano composite beam reinforced with a low content of graphene plates (GPLs) resting on an elastic foundation is investigated by Yang et al. [12]. Mohammad et al. [13] presented the buckling analysis of FG Euler-Bernoulli nano-beam based on nonlocal elasticity. Korosh and Abolfazl [14] presented buckling behavior of FG nano-plate based on exponential shear deformation theory. In 2017, Noha et al. [15] presented a modified porosity to analysis the buckling of a porous functionally graded beam. Mitao et al. [16] presented the compressive buckling analysis of functionally graded multi-layer grapheme nano platelet (GPL) polymer composite plate with in the frame work of the first shear theory of deformation. Kahya and Turan [17] developed FE design for the buckling and vibration analysis of FGB based on the first shear theory of deformation.

In 2018, Atteshamuddin and Yuwaraj [18] developed and applied a simple modified exponential shear theory of

deformation (ESDT) to analysis the buckling of graded beams with different boundary conditions.

In 2019, Ashraf et al. [19] presented buckling behavior of FG nanobeam basing on two-parameter elastic foundation dependent on shear beam theory deformation with third degree (TOSDBT). Nam et al. [20] presented a new kind of beam depended on modified shear theory deformation with first degree to study buckling behavior of FGB with different thickness.

In 2020, Farshad et al. [21] studied the buckling of various FG beam by various beam theories. To estimate the FG beam behavior, the effect of aspect ratio, material distribution, porosity index is studied. Zhicheng et al. [22] offered the dynamic analysis of buckling for FG graphene nanoplatelets (FG-GPLRC) arch subjected at its middle point to a step central point load.

The aim of this paper is to developed a new model of beam dependent on Euler, first and high order shear theory of deformation. This model of beam is used for the analysis of buckling for FG beam to demonstrate its effectiveness and accuracy.

Thus, the present paper demonstrates the buckling behavior of square FGB. The material varies along the direction of thickness by using the power law form. The motion equations of Euler and first and high order shear Timoshenko FG beam are derived using the principle of Hamilton.

2. Theory and formulation

2.1. Function Graded Beam FGB

In this study, a new FG beam model based on Euler, and shear deformation theory with first and high order is developed. This beam is modeled with length of L and square cross section of ($b \times h$) where (b) is equal to (h). Assume that the FGB is made of two different materials, ceramic and aluminum metal (E = 69 GPa, v = 0.23) in the upper and lower surface respectively as shown in Fig. 1.

Ceramic material can be determined based on the elasticity ratios that have been studied. The mechanical properties of FGB as (modulus of elasticity E (z), modulus of rigidity G (z), and Poisson ratio are varied continuously from one surface to another through the thickness direction according to the rule of mixture, it can be expressed as: [23], [24], [25].

$$P_t V_t + P_b V_b = 1 \tag{1}$$

$$V_t + V_b = 1 \tag{2}$$

$$V_t = \left(\frac{z}{h} + \frac{1}{2}\right)^k \tag{3}$$

Where (k) is non negative power law index parameter, it presented the profile of material change in thickness direction of FGB. The symbols of (t and b) represent the properties of top and bottom material when (z = h/2 and z = - h/2) respectively. The modulus of elasticity can be expressed by power law form as:

$$E(z) = (E_t - E_b)\left(\frac{z}{h} + \frac{1}{2}\right)^k + E_b \tag{4}$$

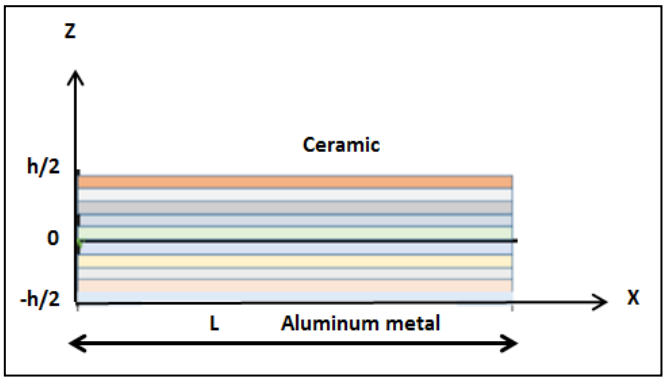

Fig. 1 geometry and loading of FG beam.

2.2. Governing Equations

In this section, the governing equations of Euler beam and first and high order Timoshenko beam are derived.

2.2.1. Timoshenko Beam Theory (TBT)

Assuming the deformations of the beam are in the x-z plane and U, V, and W, denoted to the displacement component along x, y, and z respectively. The displacement field for Timoshenko beam are taken as [26]:

$$U(x, z, t) = u(x, t) - z\frac{\partial w}{\partial x} + f(z) \times u_1(x, t) \tag{5}$$

$$V(x, z, t) = 0 \tag{6}$$

$$W(x, z, t) = w(x, t) \tag{7}$$

Where the axial and transverse middle surface displacement along X and Z direction are u (x, t) and w (x, t) respectively. The effect of transverse shear strain on the middle surface of the FGB is presented by the unknown function u_1 (x, t). The shape function is presented by f (z) that used to determine the distribution of the transverse shear strain and stress through the thickness and take deferent form as follow:

For CBT: classical beam theory (EULER): $f(z) = 0$
For FSDBT: first order shear deformation theory: $f(z) = z$
For PSDBT: parabolic or high order shear deformation theory:

$$f(z) = \frac{4z^3}{3h^2}$$

For buckling as we didn't need to kinetic energy, so we are canceled the effect of time:

The nonzero normal strains (ε_x), and (γ_{xz}) is shear strain of this beam are calculated as:

$$E_{xx} = \frac{\partial u}{\partial x} - \left(z\frac{\partial^2 w}{\partial x^2}\right) + \left(f(z)\frac{\partial u_1}{\partial x}\right) \tag{8}$$

$$\gamma_{xz} = -\frac{dw}{dx} + \left(\frac{df}{dz}u_1\right) + \frac{dw}{dx}$$

$$\gamma_{xz} = \frac{df}{dz}u_1 \tag{9}$$

By applying the principle of minimum potential energy, the variation of total potential energy (the difference between the strain energy and external work) must be equal to zero.

$$\delta \Pi = \delta (U_{int} - W_{ext}) \quad (10)$$

$$\delta(U_{int}) = \int_0^1 \left(N \times \delta \frac{du}{dx} - M \frac{d^2 w}{dx^2} + M^s \times \delta \frac{du_1}{dx} + Q^s \times \delta u_1 \right) dx \quad (11)$$

$$\delta(W_{ext}) = \int_0^1 \left\{ (q \times \delta w + f \times \delta u) + \left(P \times \frac{d^2 w}{dx^2} \times \delta w \right) \right\} dx \quad (12)$$

Where U_{int} is the strain energy, q is the distributed or concentrated load, f is the distributed axial force, P is axial component force (buckling load).

N and M are the classical well-known axial force and bending moment stress resultant, Q^s and M^s are stress resultant associated with stress deformation. These stress resultants are defined as:

$$N = \int \sigma_{xx} \, dA$$

$$M = \int z \, \sigma_{xx} \, dA$$

$$M^s = \int f_z \, \sigma_{xx} \, dA$$

$$Q^s = \int \frac{d f(z)}{dx} \sigma_{xz} \times K_s \, dA \quad (13)$$

Where K_s is the factor of shear correction and equal to (5/6), but it is equal to one for high order shear deformation theory. By applying the Hooks law in eq. (13), the stress resultant is presented in term of the strain we get:

$$N = A_{11} \frac{du}{dx} - B_{11} \frac{d^2 w}{dx^2} + E_{11} \frac{du_1}{dx} \quad (14)$$

$$M = B_{11} \frac{du}{dx} - D_{11} \frac{d^2 w}{dx^2} + F_{11} \frac{du_1}{dx} \quad (15)$$

$$M^s = E_{11} \frac{du}{dx} - F_{11} \frac{d^2 w}{dx^2} + H_{11} \frac{du_1}{dx} \quad (16)$$

$$Q^s = A_{55} \, u_1 \, K_s \quad (17)$$

Where,

$$A_{55} = \int G_z \frac{d f(z)^2}{dx} \, dA$$

$$\begin{pmatrix} N \\ M \\ M^s \\ Q^s \end{pmatrix} = \begin{pmatrix} A_{11} & B_{11} & E_{11} & 0 \\ B_{11} & D_{11} & F_{11} & 0 \\ E_{11} & F_{11} & H_{11} & 0 \\ 0 & 0 & 0 & A_{55} \end{pmatrix} \times \begin{pmatrix} \frac{du}{dx} \\ -\frac{d^2 w}{dx^2} \\ \frac{du_1}{dx} \\ u_1 \end{pmatrix} \quad (18)$$

Where,

$$(A_{11}, B_{11}, D_{11}, E_{11}, F_{11}, H_{11}) = \int E_z \, (1, Z, Z^2, f_z, (z f_z), f_z^2) \, dA \quad (19)$$

For buckling problem, the external load q and f are set to zero. By substitute equations (11) and (12) into equation (10), we get:

$$\int_0^1 \left\{ \left(N \delta \frac{du}{dx} - M \frac{d^2 w}{dx^2} + M^s \delta \frac{du_1}{dx} + Q^s \delta u_1 \right) + \left(P \frac{d^2 w}{dx^2} \delta w \right) \right\} dx = 0 \quad (20)$$

Integrating by part and setting the coefficient δu, δw and δu_1 to zero lead to the following:

$$-\frac{dN}{dx} = 0 \quad (21)$$

$$-\frac{d^2 M}{dx^2} + P \frac{d^2 w}{dx^2} = 0 \quad (22)$$

$$\frac{dM^s}{dx} - Q = 0 \quad (23)$$

All equations of motion can be obtained in terms of displacement by substituting N, M, M^s, and Q^s from eq. (18) in to eq. (21), (22), (23) as follows:

$$A_{11} \frac{d^2 u}{dx^2} - B_{11} \frac{d^3 w}{dx^3} + E_{11} \frac{d^2 u_1}{dx^2} = 0 \quad (24)$$

$$B_{11} \frac{d^3 u}{dx^3} - D_{11} \frac{d^4 w}{dx^4} + F_{11} \frac{d^3 u_1}{dx^3} - P \frac{d^2 w}{dx^2} = 0 \quad (25)$$

$$E_{11} \frac{d^2 u}{dx^2} - F_{11} \frac{d^3 w}{dx^3} + H_{11} \frac{d^2 u_1}{dx^2} - A_{55} \, u_1 = 0 \quad (26)$$

2.2.2. Euler-Bernoulli Beam Theory

For Euler beam, $f(z)$ equal to zero and the displacement field are given as:

$$U(x, z, t) = u(x, t) - z \frac{\partial w}{\partial x} \quad (27)$$

$$V(x, z, t) = 0 \quad (28)$$

$$W(x, z, t) = w(x, t) \quad (29)$$

The normal strain (ε_x) of Euler-Bernoulli beam theory is expressed as:

$$\varepsilon_{xx} = \frac{du}{dx} - \left(z \frac{d^2 w}{dx^2} \right) \quad (30)$$

The bending moment and axial force for Euler Bernoulli beam theory can be obtained with the similar steps that was applied for Timoshenko beam theory as follow:

$$N = A_{11} \frac{du}{dx} - B_{11} \frac{d^2 w}{dx^2} \quad (31)$$

$$M = B_{11} \frac{du}{dx} - D_{11} \frac{d^2 w}{dx^2} \quad (32)$$

$$\begin{bmatrix} N \\ M \end{bmatrix} = \begin{bmatrix} A_{11} & B_{11} \\ B_{11} & D_{11} \end{bmatrix} \begin{bmatrix} \dfrac{du}{dx} \\ -\dfrac{d^2w}{dx^2} \end{bmatrix} \tag{33}$$

The equations of motion can be obtained in terms of the displacements by substituting for N, M from eq. (31) and (32) in eq. (21) and (22) as follow:

$$A_{11}\frac{d^2u}{dx^2} - B_{11}\frac{d^3w}{dx^3} = 0 \tag{34}$$

$$B_{11}\frac{d^3u}{dx^3} - D_{11}\frac{d^4w}{dx^4} - P\frac{d^2w}{dx^2} = 0 \tag{35}$$

3. Analytical solution for buckling problem

For simply supported FGB, the analytical solution is determined by using the Navier solution. The function of displacement is expressed as product of undetermined coefficient and known trigonometric function to satisfy the governing equation. The following displacements are assumed as [27]:

$$u(x) = \sum_{n=1}^{N} U_n \cos(\alpha x) \tag{36}$$

$$w(x) = \sum_{n=1}^{N} W_n \sin(\alpha x) \tag{37}$$

$$u_1(x) = \sum_{n=1}^{N} G_n \cos(\alpha x) \tag{38}$$

where (U_n, W_n, G_n) are the unknown Fourier coefficients to be determined for each n value, and $\alpha = n\,\pi/L$.

3.1. Timoshenko Beam Theory

By substitute the eq. (36), (37), (38) and their derivative in eq. (24), (25), (26), the results as following:

$$\begin{bmatrix} (-\alpha^2 A_{11}) & (\alpha^3 B_{11}) & (-\alpha^2 E_{11}) \\ (\alpha^3 B_{11}) & (-\alpha^4 D_{11} + \alpha^2 P) & (F_{11}\,\alpha^3) \\ (-\alpha^2 E_{11}) & (F_{11}\,\alpha^3) & (-\alpha^2 H_{11} - A_{ss} K_s) \end{bmatrix} \begin{bmatrix} U_n \\ W_n \\ G_n \end{bmatrix} = \begin{bmatrix} 0 \\ 0 \\ 0 \end{bmatrix} \tag{39}$$

The critical buckling load is found by setting the determinant of the coefficient matrix in equation (39) to zero. For Timoshenko beam theory the critical buckling load is obtained as:

$$P = \Big[E_{11}\,\alpha^4 (B_{11}F_{11} - E_{11}D_{11}) + B_{11}\,\alpha^2\Big(B_{11}(\alpha^2 H_{11} + K_s A_{ss}) + (\alpha^2 F_{11} E_{11})\Big) + \alpha^2 A_{11}\Big(D_{11}(\alpha^2 H_{11} + A_{ss}K_s) - (\alpha^2 F_{11}{}^2)\Big)\Big] \Big/ \Big[A_{11}(\alpha^2 H_{11} + A_{ss}K_s) - \alpha^2 E_{11}{}^2\Big] \tag{40}$$

3.2. Euler-Bernoulli Beam Theory

It should be noted that for Euler-Bernoulli beam theory the value of (G_n, H_{11}, F_{11}, E_{11}) is zero. By substituting the eq. (36) and (37) and their derivative in eq. (24) and (25) we get the following:

$$\begin{bmatrix} (-\alpha^2 A_{11}) & (\alpha^3 B_{11}) \\ (\alpha^3 B_{11}) & (-\alpha^4 D_{11} + \alpha^2 P) \end{bmatrix} \begin{bmatrix} U_n \\ W_n \end{bmatrix} = \begin{bmatrix} 0 \\ 0 \end{bmatrix} \tag{41}$$

The critical buckling load is found by setting the determinant of the coefficient matrix in equation (46) to zero. For Euler FGB theory, the critical buckling load is obtained as:

$$P = \alpha^2 (A_{11} D_{11} - B_{11}{}^2)/A_{11} \tag{42}$$

4. Finite element method

Two-dimensional simple supported beam with ten layers is drawn in ANSYS software with element of (SHELL281). The FGB material properties changes due to the power law form in thickness direction. It has eight nodes with six degrees of freedom at each node: translations in the x, y, and z directions, and rotations about the x, y, and z-axes as shown in Fig. 2 (a).

SHELL281 is well-suited for linear, large rotation, and/or large strain nonlinear applications. Also, its accounts for follower (load stiffness) effects of distributed pressures.

SHELL281 can be used for layered applications for modeling composite shells or sandwich construction. The accuracy in modeling composite shells is governed by the first order shear-deformation theory (usually referred to as Mindlin-Reissner shell theory). The element formulation is based on logarithmic strain and true stress measures. The element kinematics allow for finite membrane strains (stretching). However, the curvature changes within a time increment are assumed to be small [28].

In this model there were ten layers and about (2500-8500) elements and the number of nodes were about (6370-25000) nodes as shown in Fig. 2 (b).

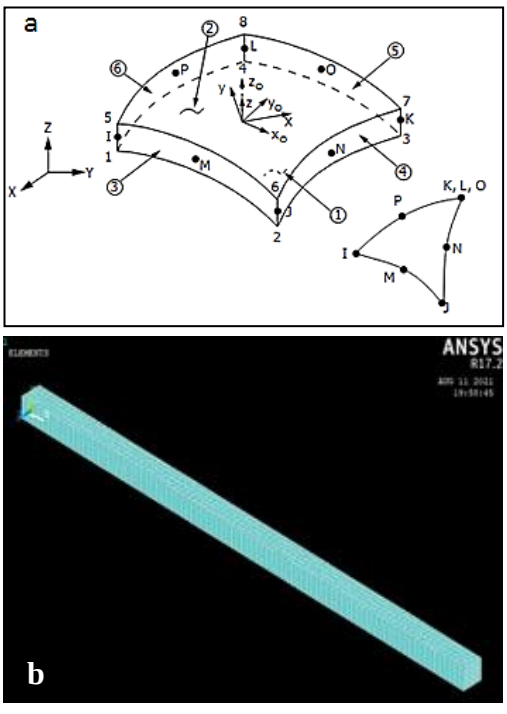

Fig. 2 (a) Element Geometry, (b) Meshing of FG Beam.

5. Numerical results and discussion

5.1. Verification

To verify the proposed beam models, the comparison among present models (analytical and numerical models) with Simsek and Yurtcu [27] and Farhatnia and Sarami [29] is investigated.

Considering a simply support beam with length L = 1 m, under concentrated load p_o, and material properties of metal in the bottom surface and alumina in top surface are [29]:

Al (metal): E_b = 70 GPa, ν_b = 0.23, ρ_b = 2700 kg/m^3

Al_2O_3(alumina): E_t = 380 GPa, ν_t = 0.23, ρ_t = 3800 kg/m^3

The dimensionless buckling of FG beam is given by [27]:

$$\widetilde{P} = \frac{PL^2}{E_b I} \tag{43}$$

The dimensionless critical buckling load for simple supported FGB of present work is compared with Simsek and Yurtcu [27] and Farhatnia and Sarami [29] as shown in Tables 1 and 2, when the power index and aspect ratio are equal to (0, 0.5, 1, 2, 5, 10) and (5 and 10) respectively.

Table 1. Validation for dimension less critical buckling load of *S-S* FGB when L/H = 5.

Authors	Index (k) for Eq. (3)					
	0	0.5	1	2	5	10
EBT [29]	53.58	34.73	26.7	20.84	17.62	16.05
RSDT [29]	48.83	31.97	24.68	19.24	16.03	14.43
RZT [29]	48.98	34	26.64	20.93	17.77	16.25
EBT [27]	53.5235	34.6962	26.67831	20.81757	17.60485	16.0354
TBT [27]	48.7882	31.9364	24.66323	19.22642	16.00867	14.4133
Present (EBT)	53.5235	34.6962	26.67831	20.81757	17.60485	16.0354
Present (TBT or FSDBT)	48.7882	31.9364	24.66323	19.22642	16.00867	14.4133
Present (HSDBT)	47.7931	33.3180	28.10264	20.94933	17.47448	16.2190
Present ANSYS	49.3478	32.2157	25.4539285	19.637142	16.521428	14.3335

Table 2. Validation for dimension less critical buckling load of *S-S* FGB when L/H = 10.

Authors	Index (k) for Eq. (3)					
	0	0.5	1	2	5	10
EBT [29]	53.57	34.73	26.7	20.83	17.62	16.05
RSDT [29]	52.31	33.99	26.17	20.41	17.19	15.61
RZT [29]	52.1	34.58	26.76	20.96	17.78	16.25
EBT [27]	53.52355	34.6962	26.67831	20.81757	17.60485	16.03548
TBT [27]	52.25561	33.96248	26.14429	20.39559	17.17669	15.59666
Present (EBT)	53.52355	34.6962	26.67831	20.81757	17.60485	16.03548
Present (TBT or FSDBT)	52.25561	33.96248	26.14429	20.39559	17.17669	15.59666
Present (HSDBT)	52.29988	33.34747	28.12501	23.96894	19.50194	16.25473
Present ANSYS	53.988	33.84171	26.29028	20.57485	16.82245	15.15223

From Tables (1) and (2), it can be found the following points:

1. For EBT, the present model is very close to the model of Simsek and Yurtcu [27] and Farhatnia and Sarami [29]. The maximum percentage of discrepancy is (0.107 %) when the power law index is (2) for any (L/H) ratio.
2. For FSDBT or TBT, the maximum percentage of discrepancy between the present model and Farhatnia and Sarami [29] is (0.133 %) for any (L/H) ratio. While that results are very close to the results of Simsek and Yurtcu [27] for all (L/H) ratio.
3. For HSDBT, the maximum percentage of discrepancy between the present study and Farhatnia and Sarami [29] are (5.2 % and 8.8 %) at (5 and 10) L/H ratio respectively.
4. For ANSYS model, the maximum percentage of discrepancy between present ANSYS model comparing with EBT, RSDT, and RZT of Farhatnia and Sarami [29] are (10.6, 3.1, and 10.6) % at L/H is (5) and (5.5, 3.2, 6.7) % at L/H ratio (10) when the power law index is (0, 0.5, 1, 2, 5, and 10) respectively. From these results may be conclude that the ANSYS of present model is very close to the RSDT of Farhatnia and Sarami [29].

From the previous comparisons, the present analytical and numerical models give a very good agreement with available literatures.

5.2. Results

The dimensionless critical buckling load of simply support FGB with different power index value (k = 0, 0.1, 0.2, 0.4, 0.6, 0.8, 1, 5, 10, 20, 30, 50 and 10000), different (L/H) ratio (5, 10, 20, 50 and 100), and with different modules ratio (0.25, 0.3333, 0.5, 0.75, 1, 1.3333, 2, 3 and 4) is calculated in this section. The lower layer of the graded beam is made up of aluminum metal. As for the properties of the rest of the layers, they are calculated based on the modulus ratios studied.

To illustrate the effect of L/H ratio on dimensionless critical buckling load of FGB based on CBT for different modulus ratio. Fig. 3 shows that the aspect ratio has not effect on the non-dimension buckling. But, by TBT that is a great effect of L/H ratio on the dimensionless buckling as shown in Fig. 4. Generally, from these figures can be determined that with increasing L/H ratio at all value of modulus ratio, the non-dimension critical buckling load increases.

To present the effect of modulus ratio (modulus of top material / modulus of bottom material) and power law index on non-dimension critical buckling load of FGB with different four present models and all L/H ratio, Figures 5 to 9 show that the dimensionless buckling increase when the modulus ratio increases at the same value of power index and by using all theories. When the value of modulus ratio is less than one, the modulus of top material (ceramic) is smaller than that of bottom material (Aluminum metal) and any increasing in power index leads to increase the value of modulus of elasticity and increase the dimensionless buckling. In the other hand when the modulus ratio is greater than one, the modulus of top material is greater than that of bottom material and any increasing in power index lead to decrease the modulus of elasticity and then decrease the dimensionless buckling. This is due to the fact that the large value of index lead to rich metal in comparison with ceramic, this make FGB more flexible.

Figures 10 to 14 illustrate the effect of the four present deformation theory on dimensionless buckling with different value of power index and different value L/H ratio. From these results it can be seen that the dimensionless buckling of CBT is greater than that of TBT and HSDBT. Its mean that the shear deformation theory lead to decrease the dimensionless critical buckling load. It can be seen also the results of ANSYS program are very close to the TBT that have been derived in this study.

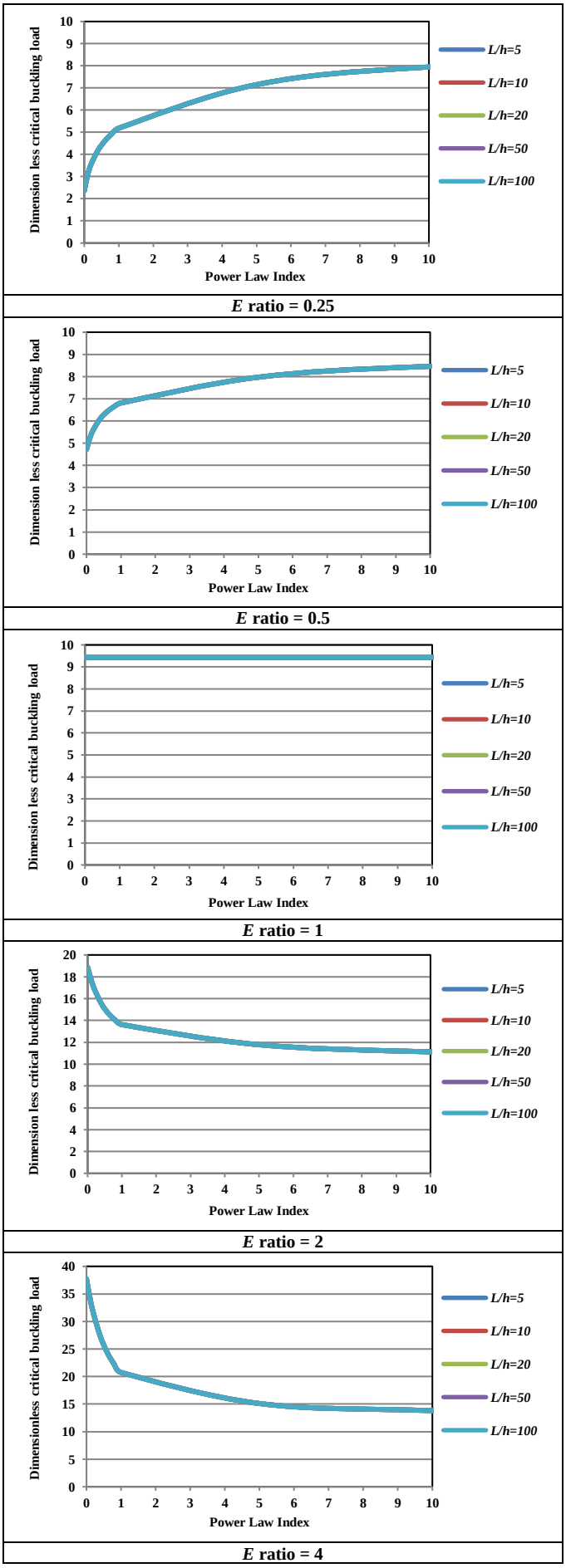

Fig. 3 The dimensionless critical buckling load of FG beam with different *L*/*H* ratio for CBT.

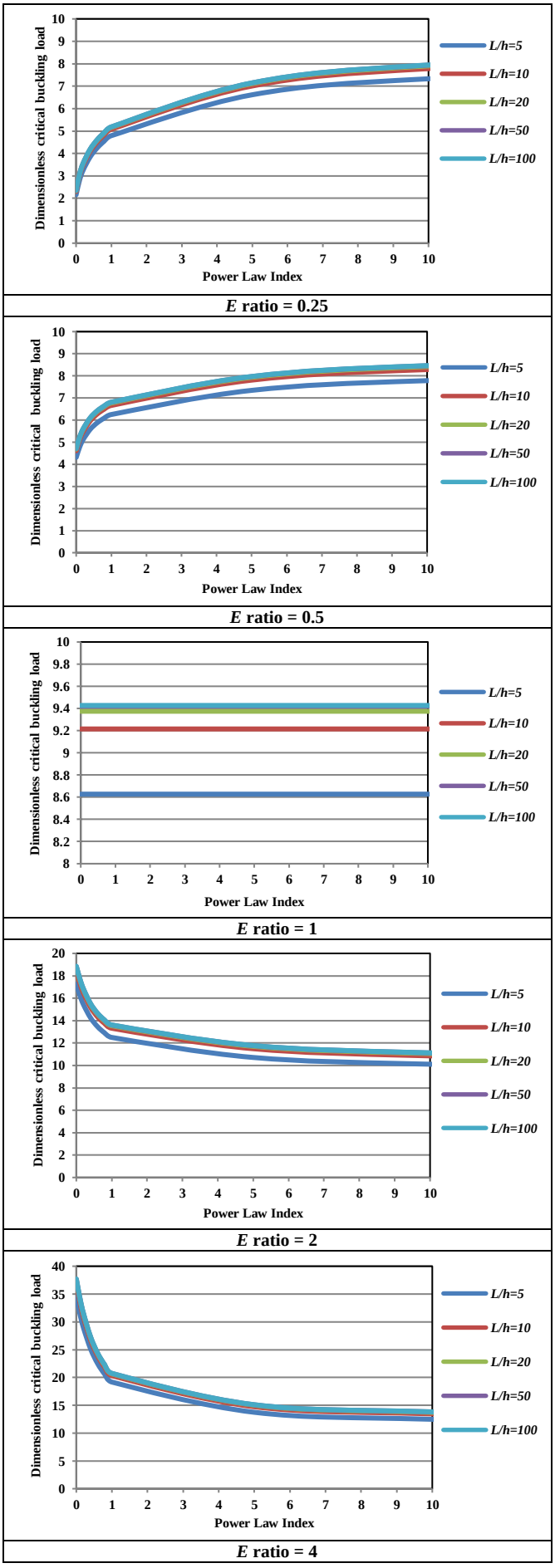

Fig. 4 The dimensionless critical buckling load of FG beam with different *L*/*H* ratio for TBT.

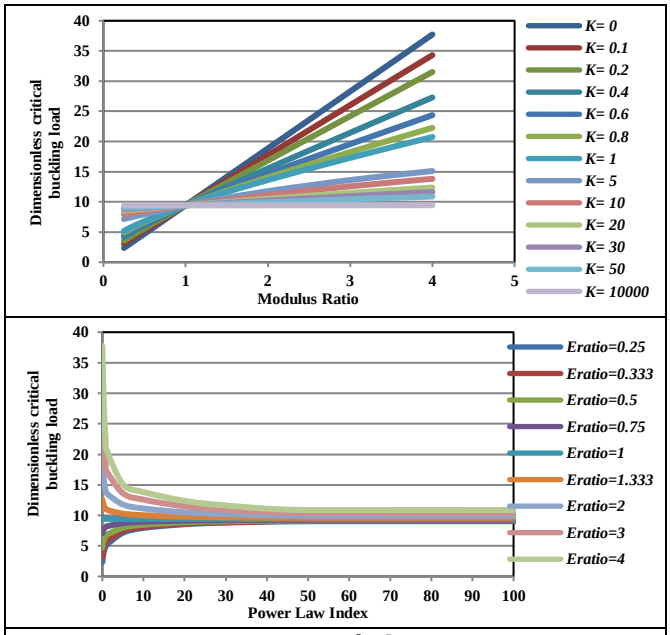

Present work- CBT

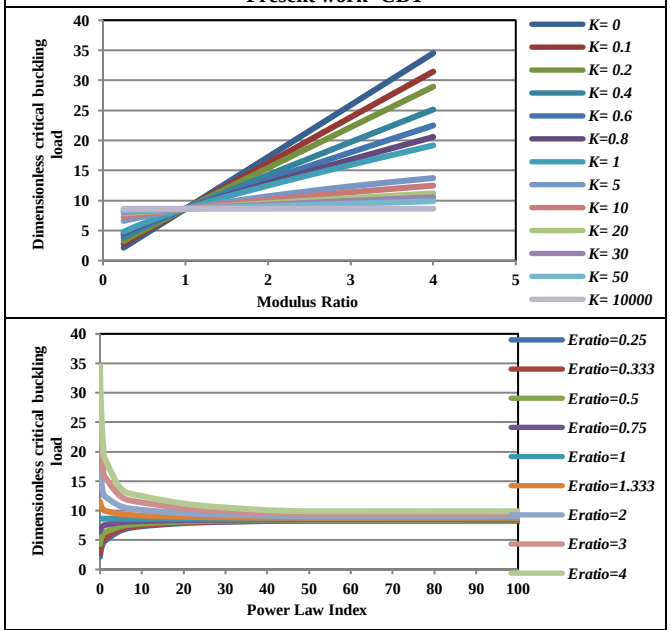

TBT

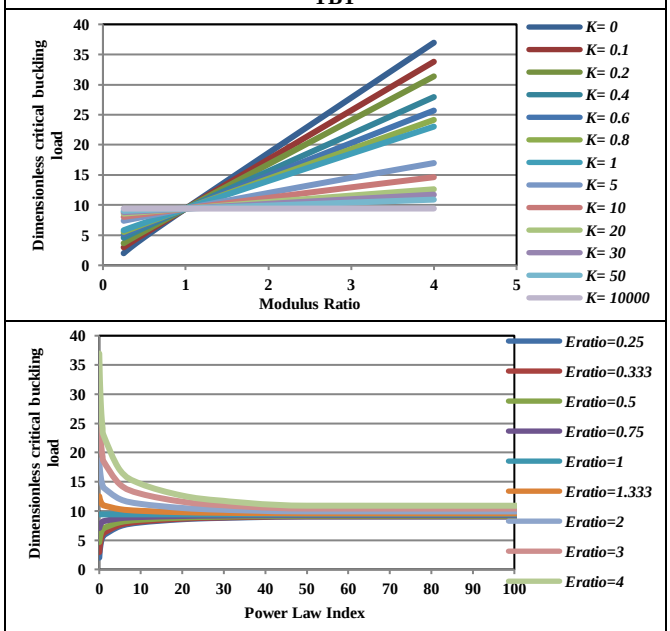

HOSDT

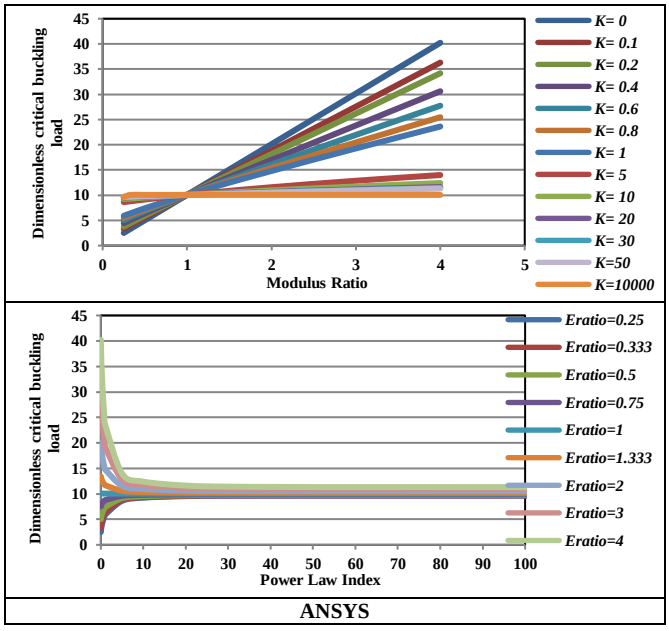

ANSYS

Fig. 5 The effect of modulus ratio and power index dimensionless critical buckling load of FG beam with (L/H = 5) and all theories.

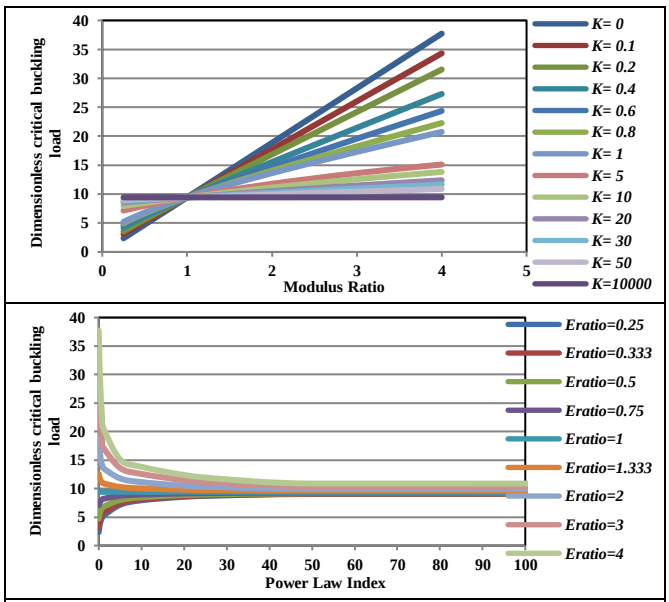

CBT

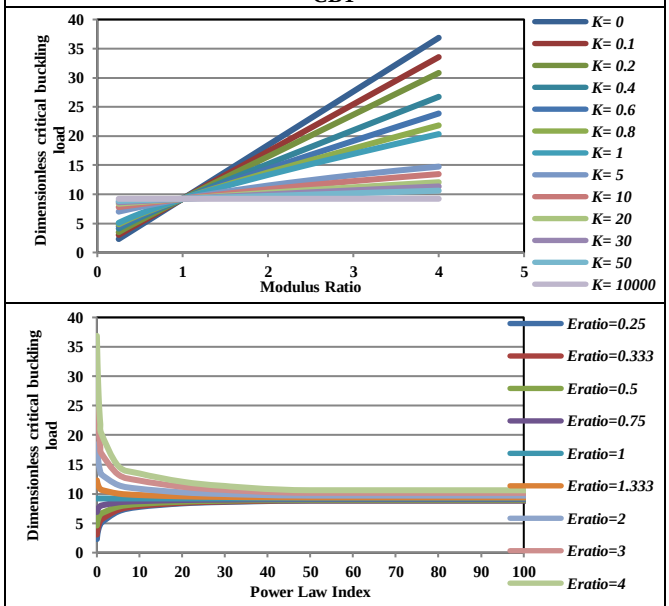

TBT

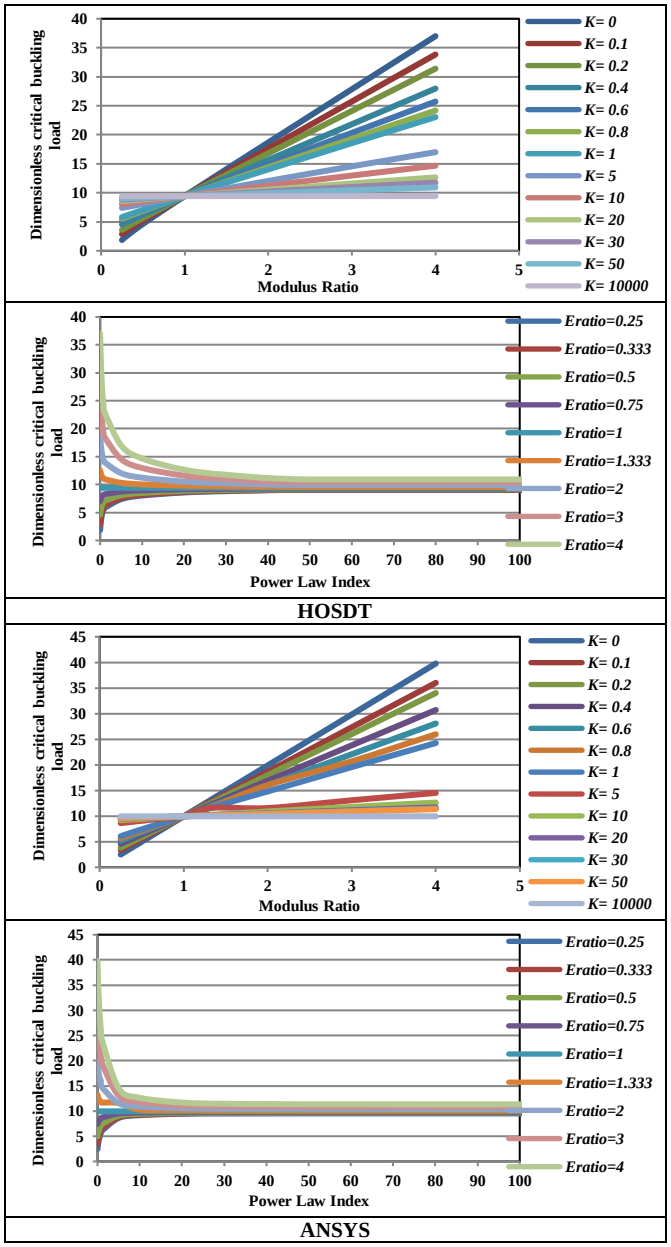

Fig. 6 The effect of modulus ratio and power index on dimensionless critical buckling load of FG beam with aspect ratio 10 and all theories.

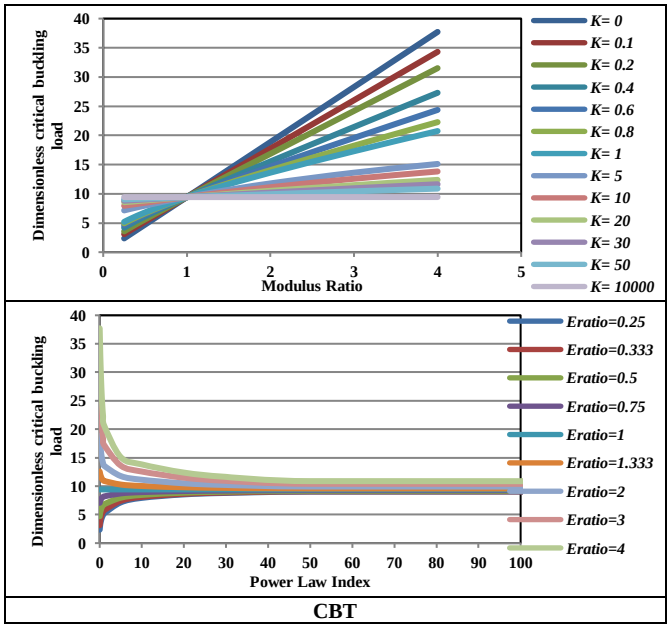

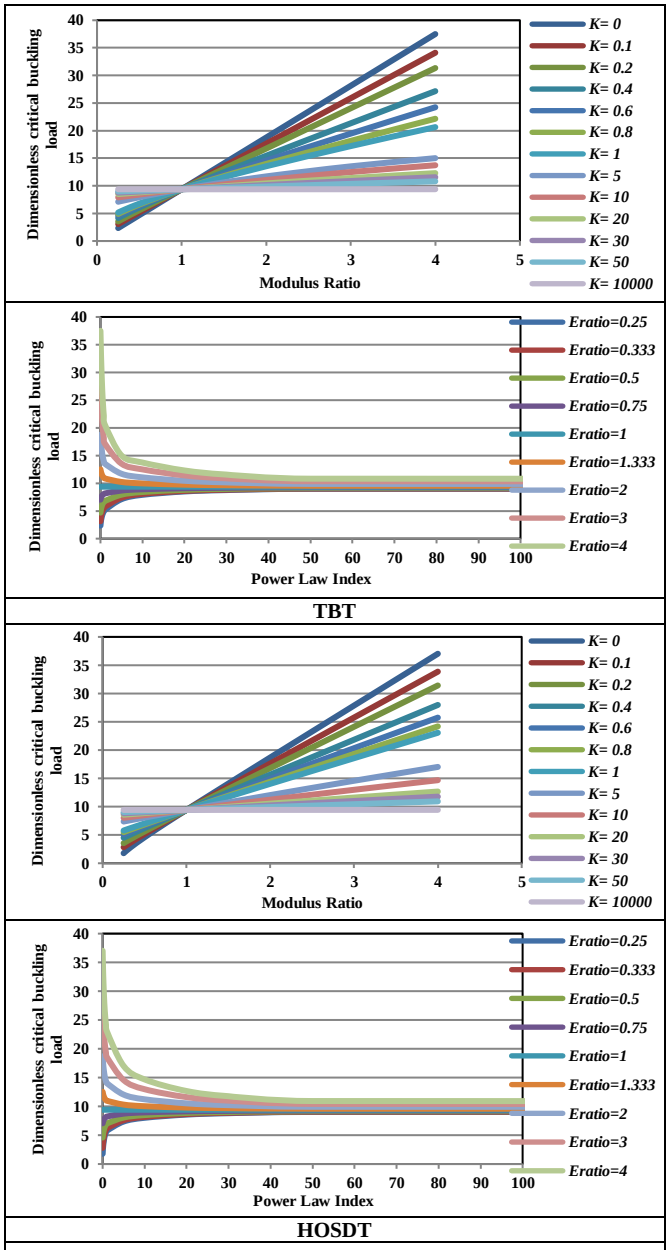

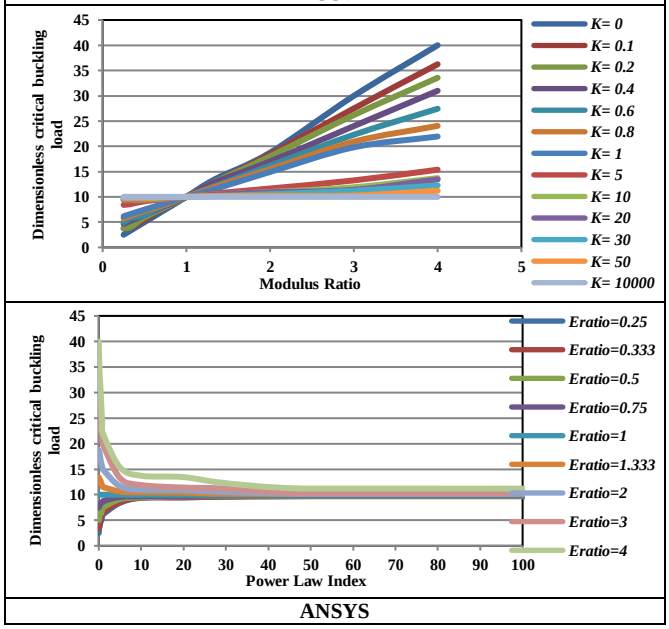

Fig. 7 The effect of modulus ratio and power index on dimensionless critical buckling load of FG beam with aspect ratio 20 and all theories.

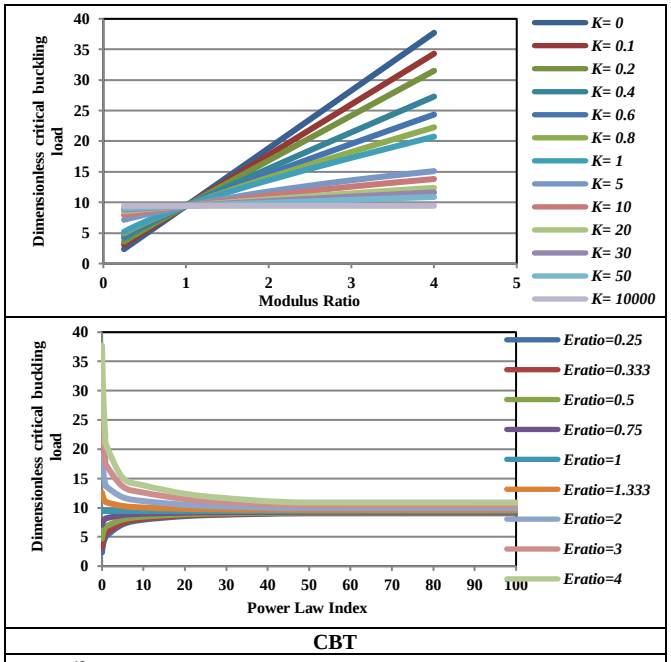

CBT

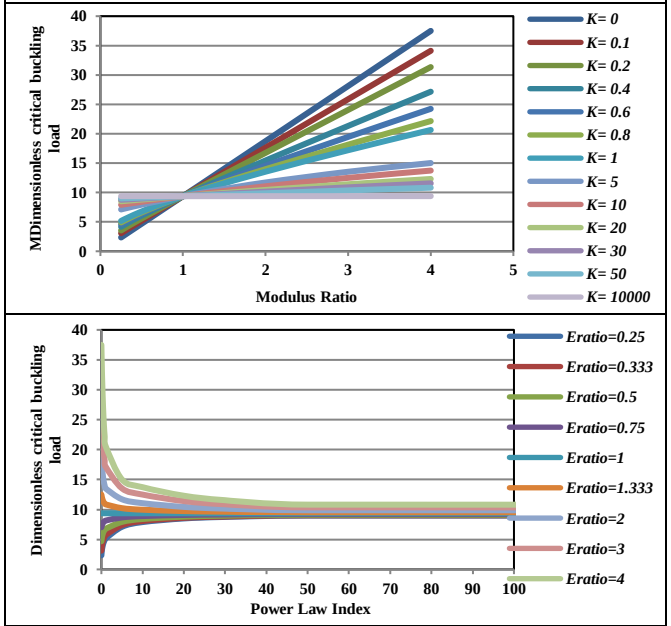

TBT

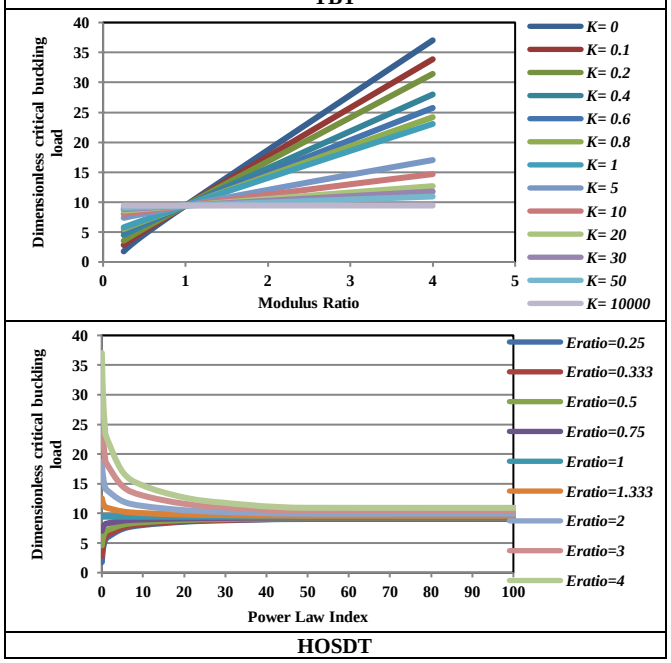

HOSDT

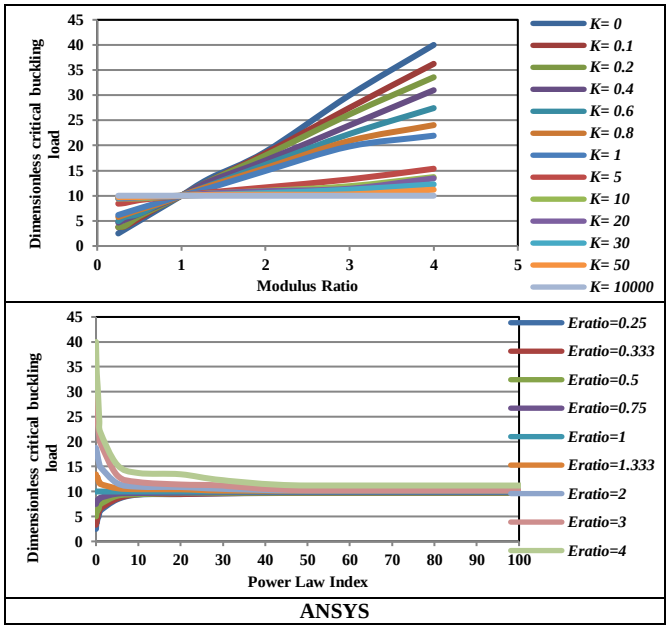

ANSYS

Fig. 8 The effect of modulus ratio and power index on dimensionless critical buckling load of FG beam with aspect ratio 50 and all theories.

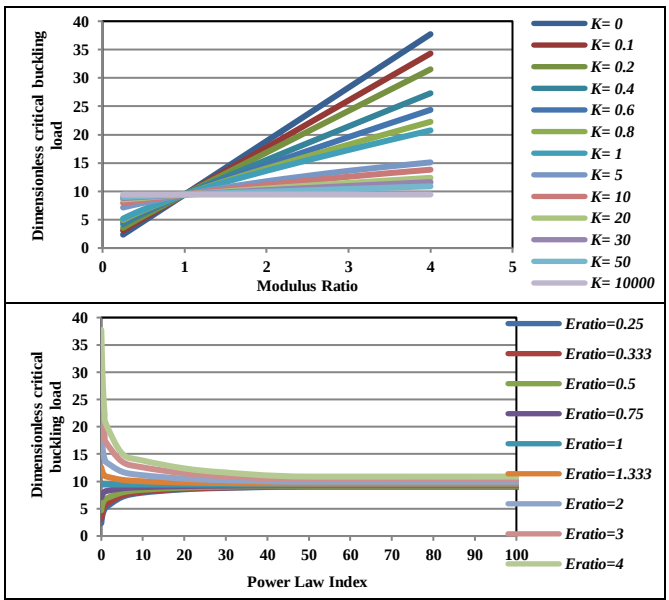

CBT

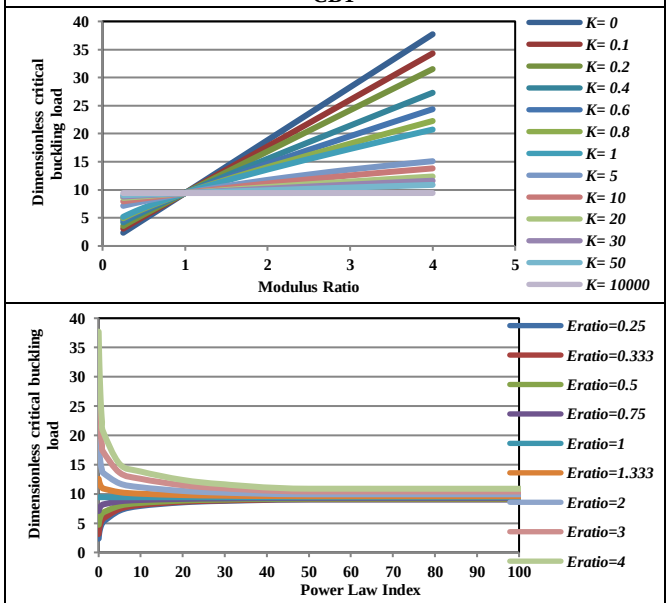

TBT

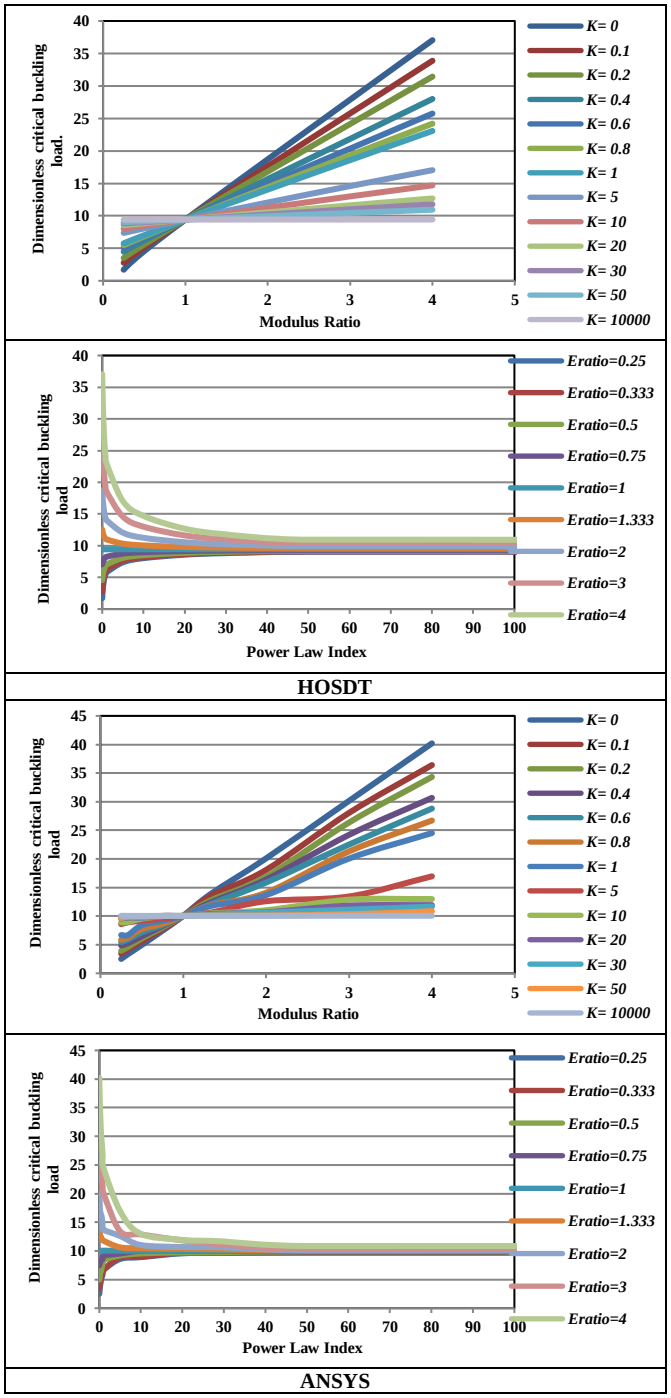

Fig. 9 The effect of modulus ratio and power law index on dimensionless critical buckling load of FG beam with aspect ratio 100 and all theories.

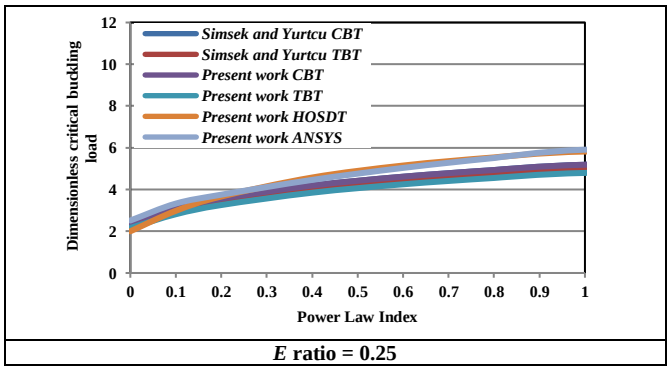

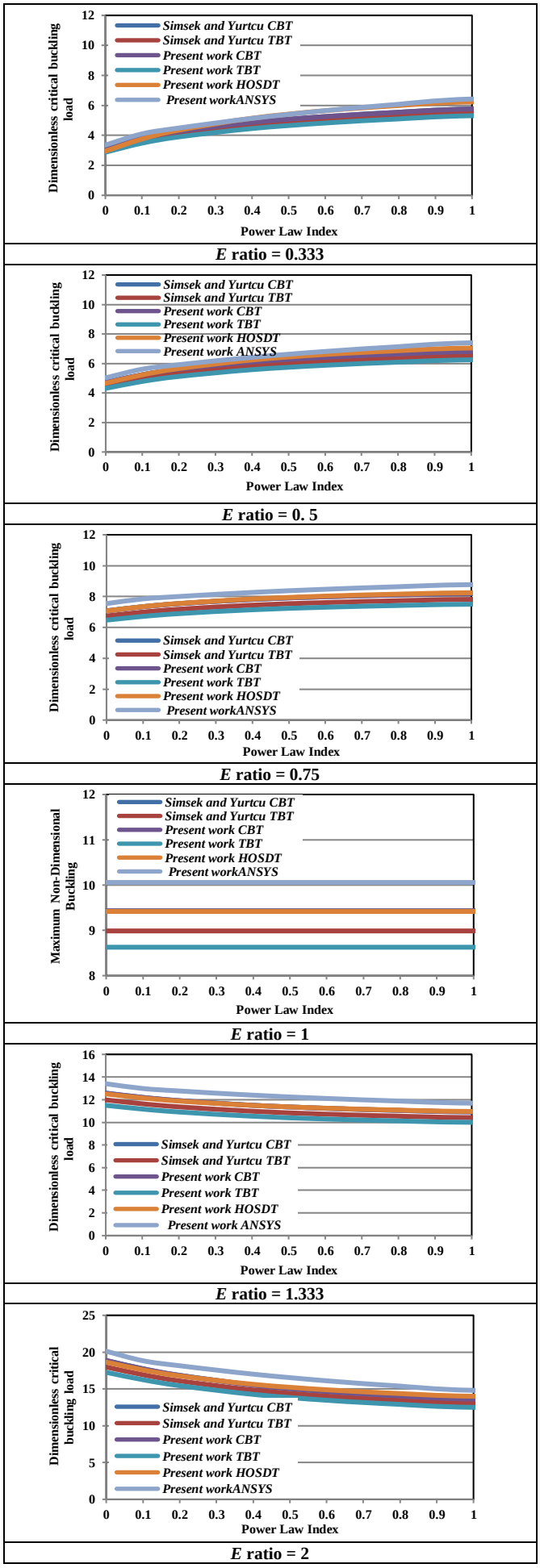

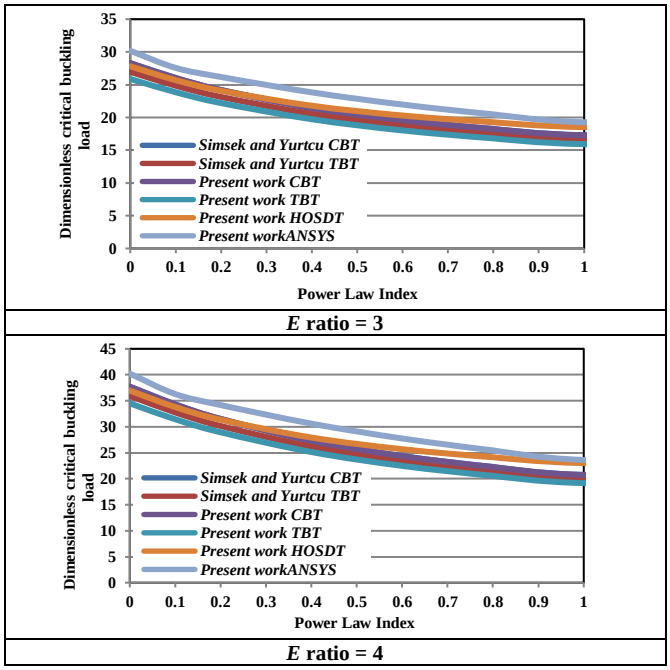

Fig. 10 The dimensionless critical buckling load of FG beam with (L/H = 5) for all theories.

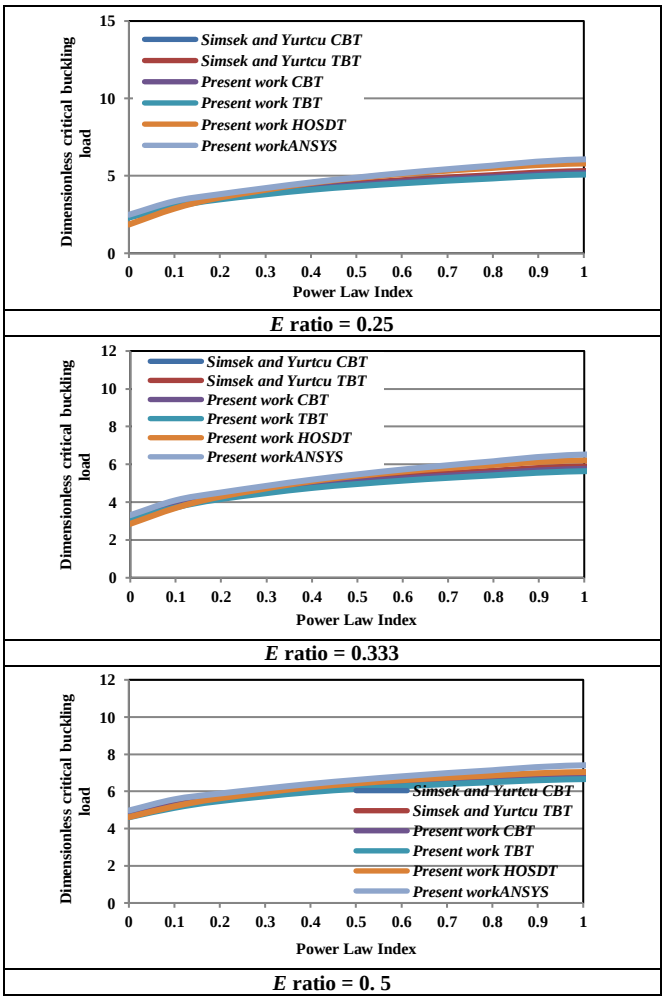

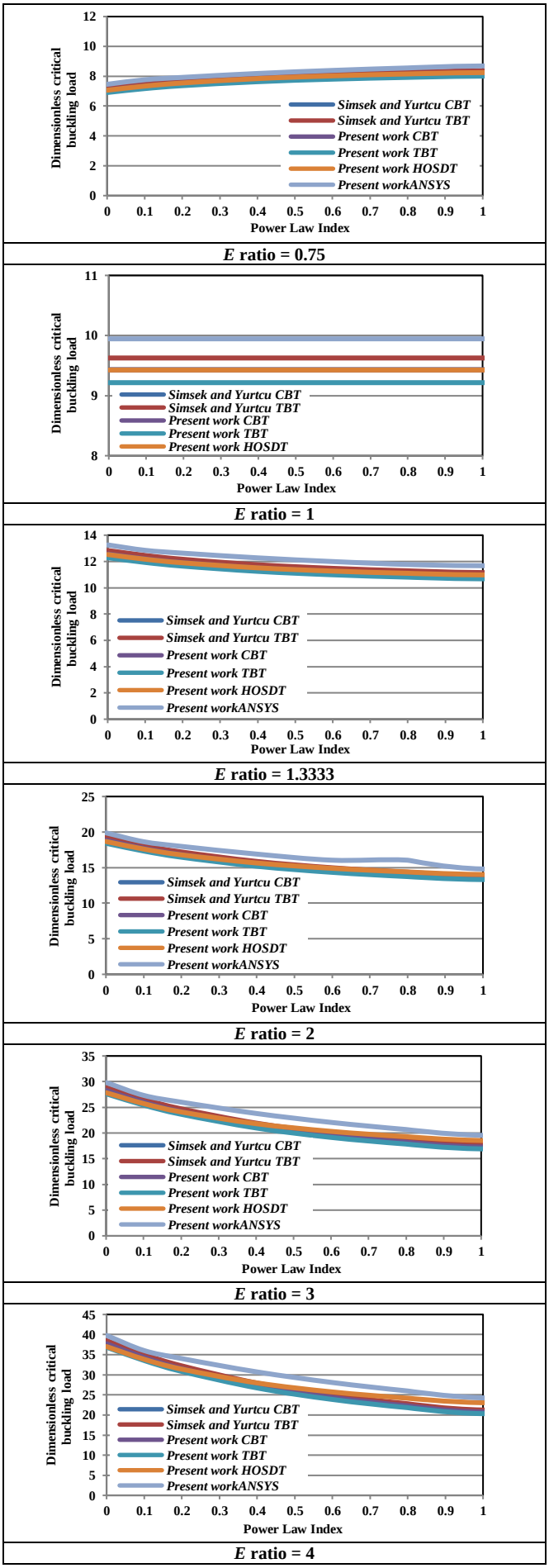

Fig. 11 The dimensionless critical buckling load of FG beam with (L/H = 10) for all theories.

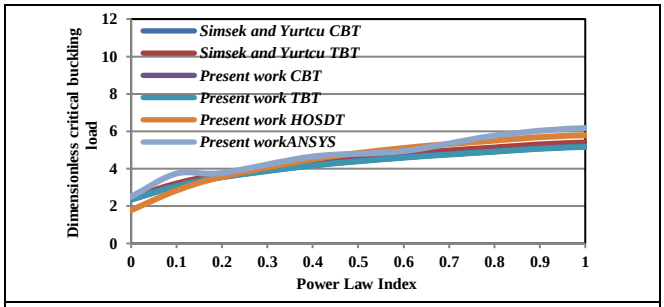

E ratio = 0.25

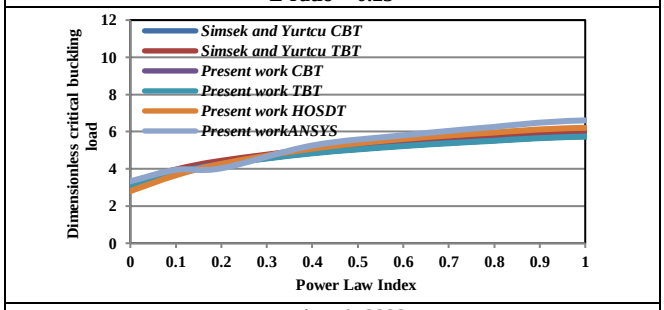

E ratio = 0. 3333

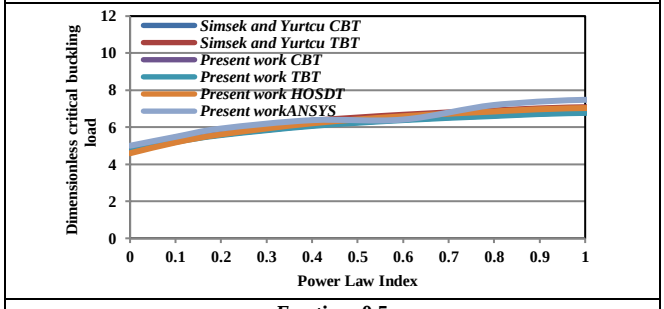

E ratio = 0.5

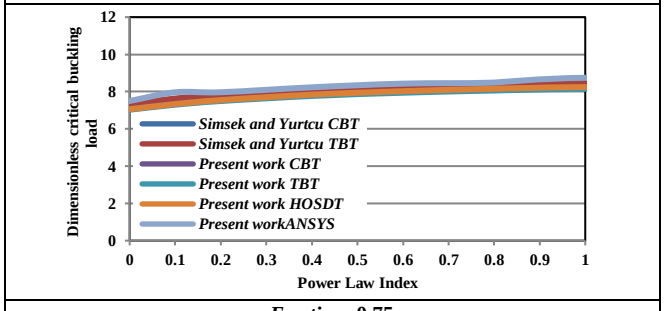

E ratio = 0.75

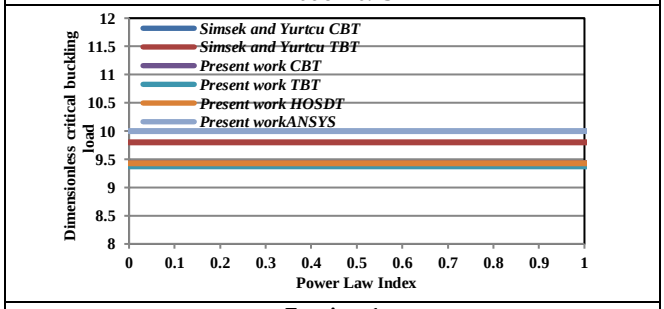

E ratio = 1

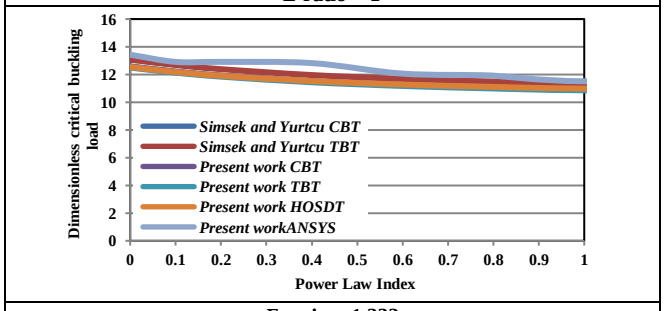

E ratio = 1.333

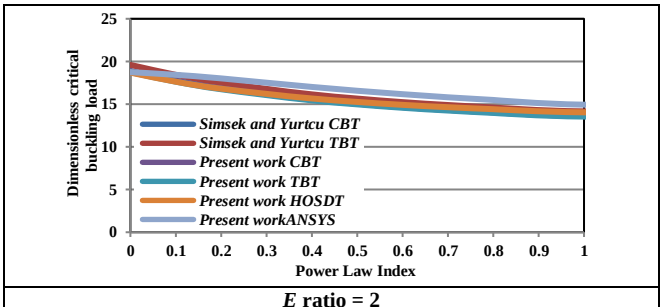

E ratio = 2

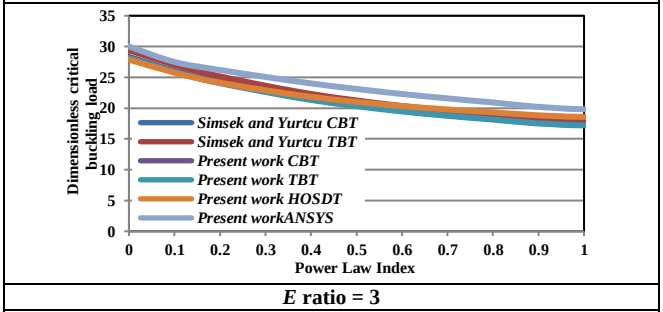

E ratio = 3

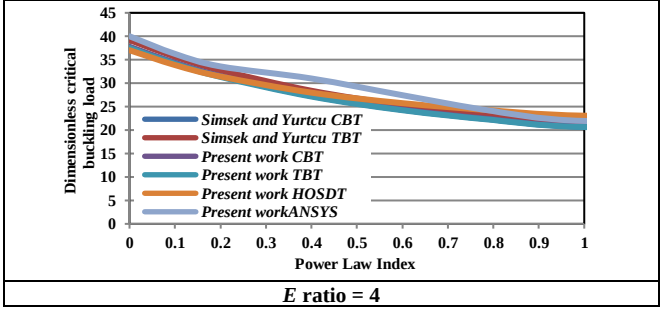

E ratio = 4

Fig. 12 The dimensionless critical buckling load of FG beam under with (L/H = 20) for all theories.

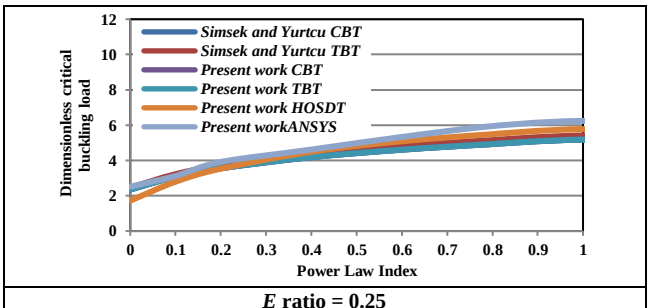

E ratio = 0.25

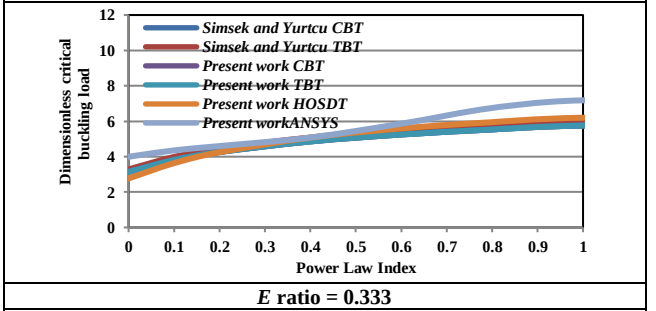

E ratio = 0.333

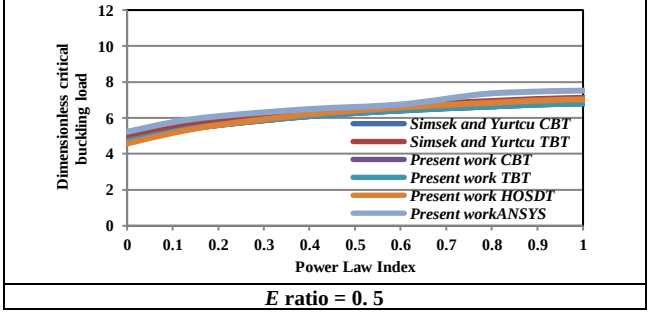

E ratio = 0. 5

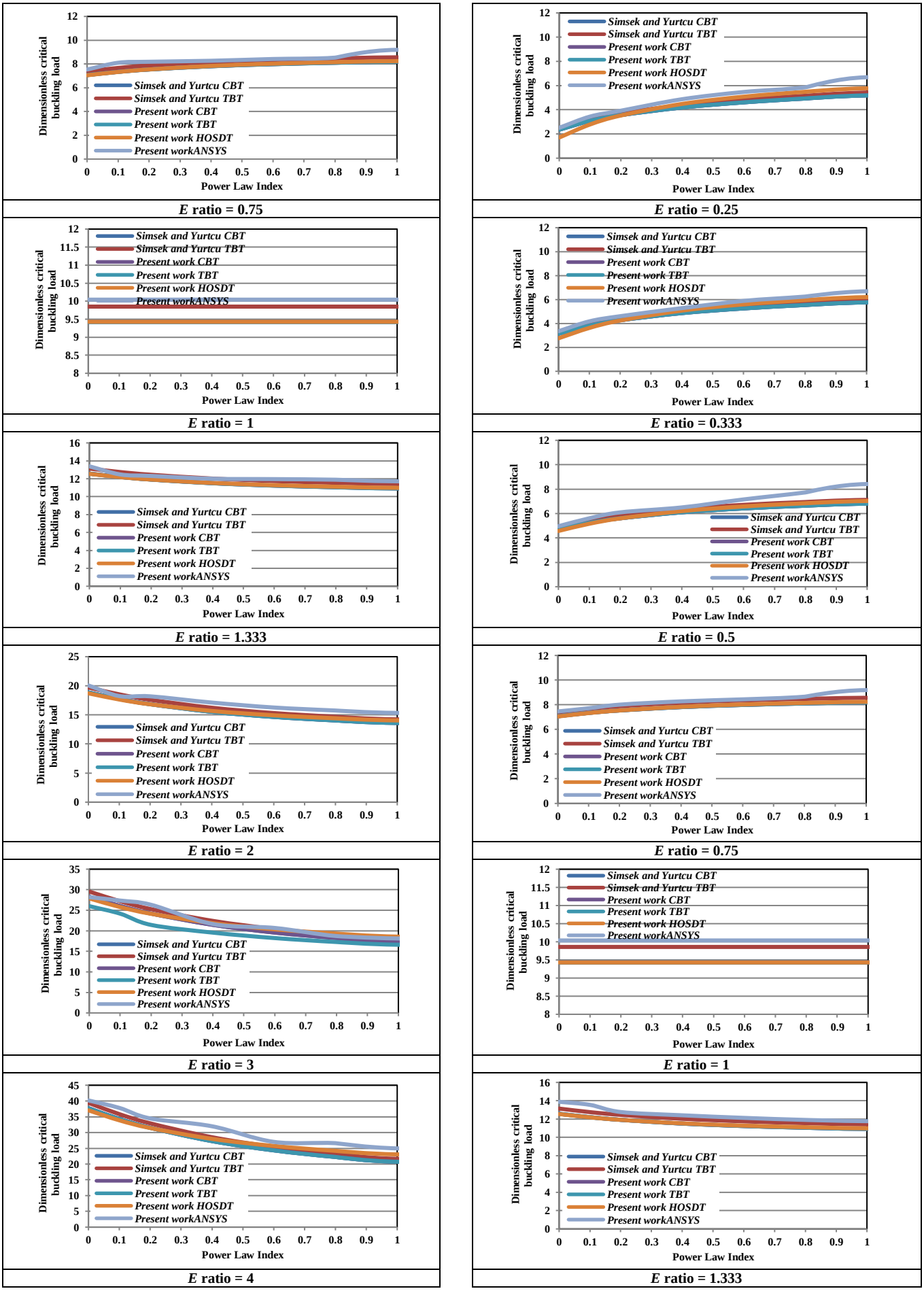

Fig. 13 The dimensionless critical buckling load of FG beam with (L/H = 50) for all theories.

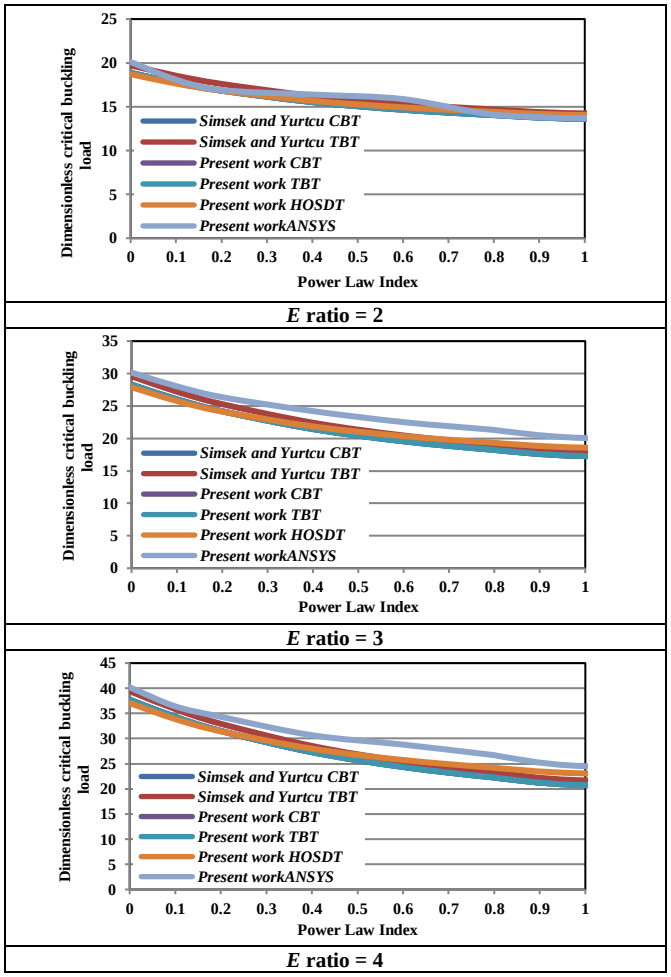

Fig. 14 The dimensionless critical buckling load of FG beam with (L/H = 100) for all theories.

6. Conclusions

In the present paper, the shear deformation Timoshenko beam theory with first and high order degree was derived. The non-dimension critical buckling load is investigated and simulated analytically and numerically. This FGB model can be analysis the buckling behavior by make a comparison between its results and the numerical results from ANSYS software and with the other published paper. Several parameters such as power index, L/H ratio, different types of deformation theories and different E ratio on non-dimension critical buckling load are studied. From the above results, we can conclude the following:

1. When the value of power law index remains constant, the dimensionless critical buckling load will increase when the elasticity ratio increase.
2. As the power law index increases, the dimensionless critical buckling load increases when the modulus ratio is less than one, decrease when the modulus ratio is greater than one, and remain constant when modulus ratio equal to one.
3. The ratio of length to thickness does not have any effect in the case of the CBT, but its effect is clear in the case of TBT that have been derived in this study.
4. The dimensionless critical buckling load increases with increasing the length to thickness ratio in TBT that have been derived in this study.
5. The results of the ANSYS program are very close to TBT that have been derived in this study.
6. The laws of dimensionless critical buckling load in the research Simsek and Yurtcu [27] were programmed in the Fortran program for the present work according to the studied modulus ratios, and the results were close to the theorems that were derived and obtained from this study.

References

[1] B. A. Samsam Shariat, and M. R. Eslami, “Buckling of thick functionally graded plates under mechanical and thermal loads”, Composite Structures, Vol. 78, pp. 433-439, 2007. https://doi.org/10.1016/j.compstruct.2005.11.001

[2] M. Aydogdu, “A general nonlocal beam theory: Its application to nanobeam bending, buckling and vibration”, Physica E: Low-dimensional Systems and Nanostructures, Vol. 41, Issue 9, pp. 1651-1655, 2009. https://doi.org/10.1016/j.physe.2009.05.014

[3] F. Farhatnia, M. A. Bagheri, and A. Ghobadi, “Buckling Analysis of FGM Thick Beam under Different Boundary Conditions using GDQM”, Advanced Materials Research, Vol. 433-440, pp. 4920-4924, 2012. https://doi.org/10.4028/www.scientific.net/AMR.433-440.4920

[4] S. R. Li and R. C. Batra, “Relations between buckling loads of functionally graded Timoshenko and homogeneous Euler-Bernoulli beams”, Composite Structures, Vol. 95, pp. 5-9, 2013. https://doi.org/10.1016/j.compstruct.2012.07.027

[5] T. K. Nguyen, T. P. Vo, and H. T. Thai, “Static and free vibration of axially loaded functionally graded beams based on the first-order shear deformation theory”, Composites Part B: Engineering, Vol. 55, pp. 147-157, 2013. https://doi.org/10.1016/j.compositesb.2013.06.011

[6] Z. X. Lei, K. M. Liew, J. L. Yu, “Buckling analysis of functionally graded carbon nanotube-reinforced composite plates using the element-free kp-Ritz method”, Composite Structures, Vol. 98, pp. 160-168, 2013. https://doi.org/10.1016/j.compstruct.2012.11.006

[7] J. Rychlewska, “Buckling analysis of axially functionally Graded beams”, Journal of Applied Mathematics and Computational Mechanics, Vol. 13, Issue 4, pp. 103-108, 2014. https://doi.org/10.17512/JAMCM.2014.4.13

[8] R. Saljooghi, M. T. Ahmadian, and G. H. Farrahi, “Vibration and buckling analysis of functionally graded beams using reproducing kernel particle method”, Scientia Iranica B, Vol. 21, Issue 6, pp. 1896-1906, 2014.

[9] T. Nguyen, T. T. Nguyen, T. P. Vo, and H. Thai, “Vibration and buckling analysis of functionally graded sandwich beams by a new higher-order shear deformation theory”, Composites Part B: Engineering, Vol. 76, pp. 273-285, 2015. https://doi.org/10.1016/j.compositesb.2015.02.032

[10] M. U. Uysal, and M. Kremzer, “Buckling Behaviour of Short Cylindrical Functionally Gradient Polymeric Materials”, Acta Physica Polonica A, Vol. 127, pp. 1355-1357, 2015. https://doi.org/10.12693/APhysPolA.127.1355

[11] T. P. Vo, H. T. Thai, T. K. Nguyen, F. Inam, and J. Lee, “A quasi-3D theory for vibration and buckling of functionally graded sandwich beams”, Composite Structures, Vol. 119, pp. 1-12, 2015. https://doi.org/10.1016/j.compstruct.2014.08.006

[12] J. Yang, H. Wu, and S. Kitipornchai, "Buckling and postbuckling of functionally graded multilayer graphene platelet-reinforced composite beams", Composite Structures, Vol. 161, pp. 111-118, 2017. http://dx.doi.org/10.1016/j.compstruct.2016.11.048

[13] M. Z. Nejad, A. Hadi, and A. Rastgoo, "Buckling analysis of arbitrary two-directional functionally graded Euler-Bernoulli nano-beams based on nonlocal elasticity theory", International Journal of Engineering Science, Vol. 103, pp. 1-10, 2016. https://doi.org/10.1016/j.ijengsci.2016.03.001

[14] K. Khorshidi, and A. Fallah, "Buckling analysis of functionally graded rectangular nano-plate based on nonlocal exponential shear deformation theory", International Journal of Mechanical Sciences, Vol. 113, pp. 94-104, 2016. http://dx.doi.org/10.1016/j.ijmecsci.2016.04.014

[15] N. Fouda, T. El-midany, and A. M. Sadoun, "Bending, Buckling and Vibration of a Functionally Graded Porous Beam Using Finite Elements", Journal of Applied and Computational Mechanics, Vol. 3, Issue 4, pp. 274-282, 2017. http://dx.doi.org/10.22055/JACM.2017.21924.1121

[16] M. Song, J. Yang, and S. Kitipornchai, "Bending and buckling analyses of functionally graded polymer composite plates reinforced with graphene nanoplatelets", Composites Part B: Engineering, Vol. 134, pp. 106-113, 2018. https://doi.org/10.1016/j.compositesb.2017.09.043

[17] V. Kahya, and M. Turan, "Finite element model for vibration and buckling of functionally graded beams based on the first order shear deformation theory", Composites Part B: Engineering, Vol. 109, pp. 108-115, 2017. https://doi.org/10.1016/j.compositesb.2016.10.039

[18] A. S. Sayyad, and Y. M. Ghugal, "Analytical solutions for bending, buckling, and vibration analyses of exponential functionally graded higher order beams", Asian Journal of Civil Engineering, Vol. 19, pp. 607-623, 2018. https://doi.org/10.1007/s42107-018-0046-z

[19] A. Zenkour, F. Ebrahimi, M. R. Barati, "Buckling analysis of a size-dependent functionally graded nanobeam resting on Pasternak's foundations", International Journal of Nano Dimension, Vol. 10, Issue 2, pp. 141-153, 2019. http://www.ijnd.ir/article_662465.html

[20] V. H. Nam, P. V. Vinh, N. V. Chinh, D. V. Thom and T. T. Hong, "A New Beam Model for Simulation of the Mechanical Behaviour of Variable Thickness Functionally Graded Material Beams Based on Modified First Order Shear Deformation Theory", Materials, Vol. 12, Issue 3, pp. 1-23, 2019. https://doi.org/10.3390/ma12030404

[21] F. Rahmani, R. Kamgar, and R. Rahgozar, "Finite Element Analysis of Functionally Graded Beams using Different Beam Theories", Civil Engineering Journal, Vol. 6, No. 11, pp. 2086-2102, 2020. https://doi.org/10.28991/cej-2020-03091604

[22] Z. Yang, A. Liu, J. Yang, J. Fu, and B. Yang, "Dynamic buckling of functionally graded grapheme nanoplatelets reinforced composite shallow arches under a step central point load", Journal of Sound and Vibration, Vol. 465, 2020. https://doi.org/10.1016/j.jsv.2019.115019

[23] S. M. Aldousari, "Bending analysis of different material distributions of functionally graded beam", Applied Physics A, Vol. 123, No. 296, pp. 1-9, 2017. https://doi.org/10.1007/s00339-017-0854-0

[24] A. Nateghi, M. Salamat-talab, J. Rezapour, and B. Daneshian, "Size dependent buckling analysis of functionally graded micro beams based on modified couple stress theory", Applied Mathematical Modelling, Vol. 36, Issue 10, pp. 4971-4987, 2012. https://doi.org/10.1016/j.apm.2011.12.035

[25] M. Şimşek, "Buckling of Timoshenko Beams Composed of Two-Dimensional Functionally Graded Material (2D-FGM) Having Different Boundary Conditions", Composite Structures, Vol. 149, pp. 304-314, 2016. http://dx.doi.org/10.1016/j.compstruct.2016.04.034

[26] K. Amara, M. Bouazza, and B. Fouad, "Postbuckling Analysis of Functionally Graded Beams Using Nonlinear Model", Periodica Polytechnica Mechanical Engineering, Vol. 60, No. 2, pp. 121-128, 2016. https://doi.org/10.3311/PPme.8854

[27] M. Simsek and H. H. Yurtcu, "Analytical solutions for bending and buckling of functionally graded nanobeams based on the nonlocal Timoshenko beam theory", Composite Structures, Vol. 97, pp. 378-386, 2013. https://doi.org/10.1016/j.compstruct.2012.10.038

[28] ANSYS Mechanical APDL Element Reference, ANSYS, Inc., 2016.

[29] F. Farhatnia1 and M. Sarami, "Finite Element Approach of Bending and Buckling Analysis of FG Beams Based on Refined Zigzag Theory", Universal Journal of Mechanical Engineering, Vol. 7, No. 4, pp. 147-158, 2019. https://doi.org/10.13189/ujme.2019.070402